9348-AN-c1

Transition Velocity Experiments on Ceramics

Final Technical Report
by

Patrik Lundberg

November 2003

United States Army
European Research Office of the U. S. Army
London, England

Contract number: N62558-02-M-6377

Contractor: Kevin Linden

Approved for Public Release; Distribution Unlimited

20040219 116

REPORT DOCUMENTATION PAGE

Form Approved
OMB No. 074-0188

1. AGENCY USE ONLY (Leave blank)	2. REPORT DATE 5 November 2003	3. REPORT TYPE AND DATES COVERED Final report

4. TITLE AND SUBTITLE
Transition Velocity Experiments on Ceramics

5. FUNDING NUMBERS
C - N62558-02-M-6377

6. AUTHOR(S)
Patrik Lundberg

7. PERFORMING ORGANIZATION NAME(S) AND ADDRESS(ES)

Swedish Defence Research Agency, FOI
Weapons and Protection Division
Grindsjön Research Centre
SE-147 25 Tumba
Sweden

8. PERFORMING ORGANIZATION REPORT NUMBER
FOI 02-1367

9. SPONSORING / MONITORING AGENCY NAME(S) AND ADDRESS(ES)

US Naval Regional Contracting Center,
Det London, Government Buildings,
Block 2, Wing 12, Lime Grove, Ruislip,
Middlesex HA4 8BX
United Kingdom

10. SPONSORING / MONITORING AGENCY REPORT NUMBER

11. SUPPLEMENTARY NOTES

12a. DISTRIBUTION / AVAILABILITY STATEMENT

12b. DISTRIBUTION CODE

13. ABSTRACT (Maximum 200 Words)
ARL has awarded FOI a contract to assess the transition velocities of four silicon carbide (SiC) materials of potential interest for armor applications using a test method developed at FOI. These materials are produced by Cercom Inc. and have the designations SiC B, SiC N, SiC HPN and SiC-SC-1RN.

FOI has fabricated the targets and carried out the tests required under the contract to supplement tests performed earlier at FOI. In this report, all primary data are accounted for and the penetration and erosion velocities are evaluated. The transition velocity intervals are obtained to within 50 m/s or better, enabling a ranking of the materials. SiC HPN has the highest transition velocity, above 1600 m/s, while the other materials have a transition velocity just above 1500 m/s.

The transition from interface defeat to penetration is distinct and the complicated penetration behavior above the transition velocity is discussed. Suggestions for possible additional work are presented.

14. SUBJECT TERMS
Ceramic armor, interface defeat, transition velocity, SiC

15. NUMBER OF PAGES
26

16. PRICE CODE

17. SECURITY CLASSIFICATION OF REPORT Unclassified	18. SECURITY CLASSIFICATION OF THIS PAGE Unclassified	19. SECURITY CLASSIFICATION OF ABSTRACT Unclassified	20. LIMITATION OF ABSTRACT

NSN 7540-01-280-5500

Standard Form 298 (Rev. 2-89)
Prescribed by ANSI Std. Z39-18
298-102

INTENTIONALLY LEFT BLANK.

CONTENTS

INTENTIONALLY LEFT BLANK.

1 BACKGROUND

Armour systems containing high hardness materials, e.g. high quality ceramics, can be capable of defeating armour-piercing projectiles on the surface of this hard component. This phenomenon, called interface defeat and first reported by Hauver et al, ref [1], has been investigated extensively at FOI since the middle of the 1990-ties, see e.g. ref [2-3]. During this time FOI has developed a test method by which the transition velocity, that is the velocity at which the projectile starts to penetrate the hard surface, can be assessed in a convenient way. ARL has awarded FOI a contract to assess the transition velocities of certain silicon carbide (SiC) materials of potential interest for armour applications using this test method. The four materials were produced by Cercom Inc., USA and had the designation PAD SiC-B, PAD SiC-N, PAD SiC-SC-1RN and PAD SiC-HPN. All materials were supplied by ARL apart from the SiC-B which was earlier supplied to FOI by [dstl].

The contract was awarded September 5, 2002 and runs for 14 months.

1.1 Test matrix

Some of the materials of interest to ARL in the current investigation have already been subjected to some preliminary testing at FOI. In these tests, two different covers were used: a fairly thick homogeneous steel cover and a thin copper cover with a cylinder (diameter 2 and length 4 times the diameter of the projectile) in the middle. The copper cover turned out to be the most discriminating design and thus the most effective one in assessing the (relative) transition velocities. It should be pointed out that the copper cover target design will not give the highest possible transition velocity of the investigated materials but it is the best method we have found so far to rank the materials. Up until now the following tests have been performed with the materials that ARL are interested in:

SiC-N: 10 tests; 2 using a steel cover, 7 using a copper cover (one failure)
SiC-HPN: 10 tests; 3 using a steel cover, 6 using a copper cover (one failure)
SiC-1RN: 10 tests; 4 using a steel cover, 5 using a copper cover (one failure)

The experiments within the contract were all carried out using the copper cover design. The following test matrix was used:

- Additional tests on SiC-N, SiC-HPN and SiC-1RN to determine the transition velocity to within 50 m/s.

- Determination of the transition velocity of SiC-B using the same target (copper cover) as for the above SiC materials. This added up to 21 impact experiments. 10 of these were financed under this contract and the rest by an ongoing FOI research program.

1.2 Supply of test materials and specification of work

SiC-B: FOI had a plate from the same delivery as the one used in the tests published in ref [3]. FOI produced the 10 test samples needed for the experiments.

SiC-N, SiC-HPN and SiC-1RN: ARL delivered 5 samples of each material to FOI.

FOI manufactured the complete targets, carried out and evaluated the experiments.

The experiments are focused on determining the transition velocity. Penetration versus time data evaluated from X-ray radiographs are presented together with evaluated values of penetration and erosion velocities.

2   CERAMIC MATERIALS INVESTIGATED

The silicon carbide materials were produced by Cercom Inc., USA. The impact tests were performed at two different occasions during the period 2001-2002 (FOI work) and 2003 (contract work). The materials tested during 2001-2002 and 2003 are listed in Tables 1 and 2, respectively.

Table 1 Materials used in test number 300-369 (2001)

Ceramic (tile)	Ceramic (name)
3-888-3C	PAD SiC-B
6-0052-2B	PAD SiC-N
RHP 485-2	PAD SiC-SC-1RN
RHP 485-1	PAD SiC-HPN

Table 2   Materials in test number 417-438 (2002)

Ceramic (tile)	Ceramic (name)
3-888-3B	PAD SiC-B
6-0079-5	PAD SiC-N
RHP 482-1	PAD SiC-SC-1RN
RHP 502-1	PAD SiC-HPN

A possible interchange between SiC-SC-1RN and SiC-HPN in the tests performed during 2001-2002 could have taken place. The reason for this suspicion is contradictory results when comparing series 1 and 2. Since the material SiC-HPN incorrectly was named SiC-SC-HPN during the target manufacturing for the tests 2001-2002, this could be a possible reason for such an interchange. Another reason is that the second set of materials has different mechanical properties than the first set. In other words, these sets should be handled as separate materials.

FOI has performed hardness and fracture toughness tests (using Vickers indentation technique) and density measurements in order to determine if an interchange has taken place. All these tests indicate that this is the case. Nevertheless, a more precise investigation should be done to verify that this interchange has taken place.

In this report, we assume that this interchange has taken place (this means that the results for SiC-HPN and SiC-SC-1RN should be interchanged in interim report number 2).

3   EXPERIMENTS AND EVALUATIONS

The experiments were performed using a two-stage light-gas gun and the reverse impact technique. Confined ceramic cylinders with nominal diameter 20 mm and length 20 mm were launched against a stationary projectile mounted in front of the barrel. The projectile was suspended in a block of divinycell (density 45 kg/m^3). The sintered tungsten alloy [1] projectiles (Y 925 from Kennametal Hertel AG) were cylinders with a length of 80 mm and a diameter of 2 mm. Figure 1 shows the outline of the target and the projectile.

The confinement consisted of a steel cylinder, outer diameter 28 mm and a copper cover (OFHC). The steel cylinder was made of marageing steel (Mar 350). The inner diameter of the cylinder was slightly smaller, 0.07 mm, than the diameter of the silicon carbide cylinder and the tube was heated to about 475 °C before the ceramic cylinder was inserted (shrink fit). Figure 2 shows the detailed geometry of the target confinement.

The copper cover consisted of a 0.5 mm thick circular plate with a diameter 4 mm and length 8 mm cylinder at the centre. The copper cover was glued onto the steel cylinder. The copper cover geometry is shown in detail in figure 3.
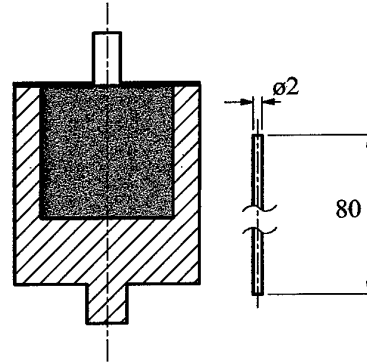

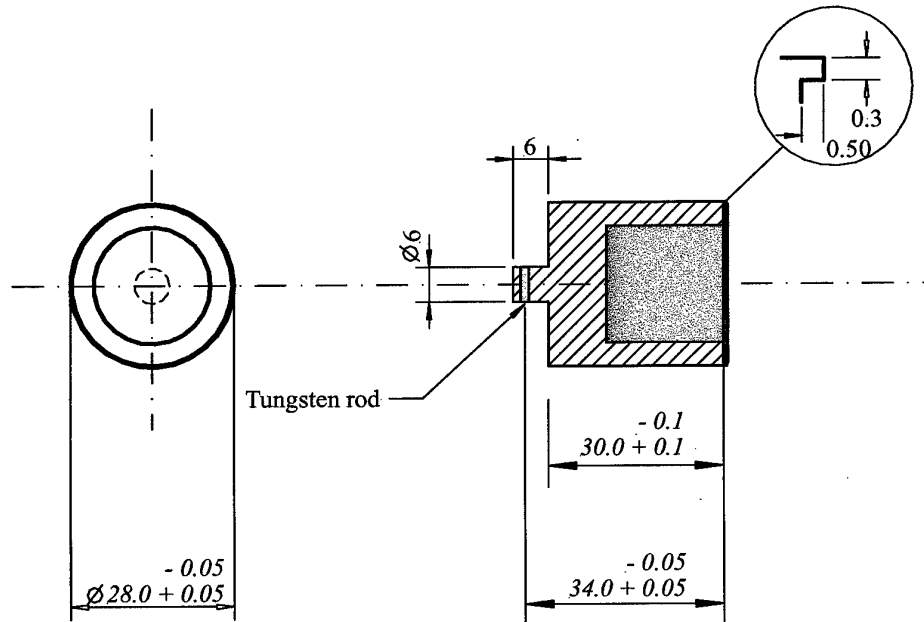Fig. 1   Target and projectile for reverse impact experiments (mm).
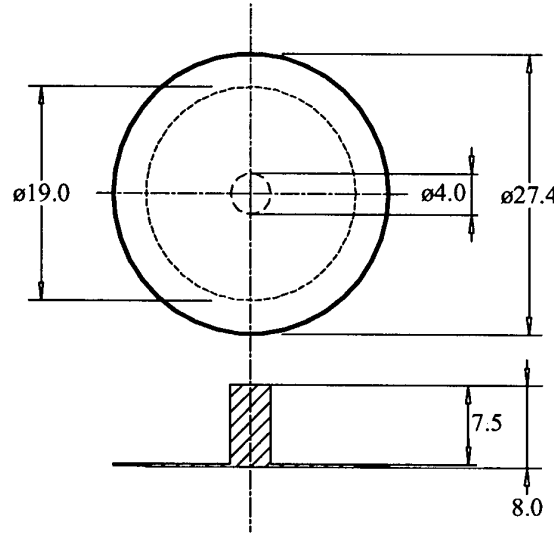

Fig. 2   Steel confinement.

Fig. 3   Copper cover.

The shrink fit gives a confining pressure p on the ceramic cylinder. The pressure can be estimated using

$$p = \frac{\delta}{R_c\left(\dfrac{(1-v_c)}{E_c} + \dfrac{(1-v_s)R_c^2 + (1+v_s)R_s^2}{E_s(R_s^2 - R_c^2)}\right)}$$

where δ is the difference in radius between the ceramic and the interior of the confinement, R is the radius, v is the Poisson's ratio and E the Young modulus. Index c and s refer to the ceramic and the steel materials, respectively. Using $\delta = 0.035$ mm, $R_c = 10$ mm, $R_s = 14$ mm, $v_c = 0.16$, $v_s = 0.3$, $E_c = 449$ GPa and $E_s = 186$ GPa gives a confining pressure of around 175 MPa.

Two 150 kV X-ray flashes were used to determine the impact velocity v_0. The first was triggered at impact and the second after the target-projectile interaction had ended. This velocity is slightly lower (10-20 m/s because of retardation due to the interaction with the projectile) than the "true" impact velocity but will be used as impact velocity henceforth. This means that the transition velocity evaluated in this report are 10-20 m/s lower than the "true" transition velocity. The X-ray pulse times were measured to within 0.1 μs. The uncertainty in the impact velocity evaluation is estimated to ±5 m/s.

Four 450 kV X-ray flashes, positioned at the same distance from the barrel and separated radially by 30°, were used to record the penetration process. The X-ray pulse times were measured to within 0.1 μs. The penetration depth P in the ceramic was determined from the X-ray pictures using image-processing techniques. The inaccuracy in the measurement of penetration depth is of the order of ± 0.20 mm.

From the flash X-ray picture data it is possible to evaluate the penetration velocity u and the projectile erosion velocity $\dot{L}$. The experimental set-up is shown in Fig. 4.
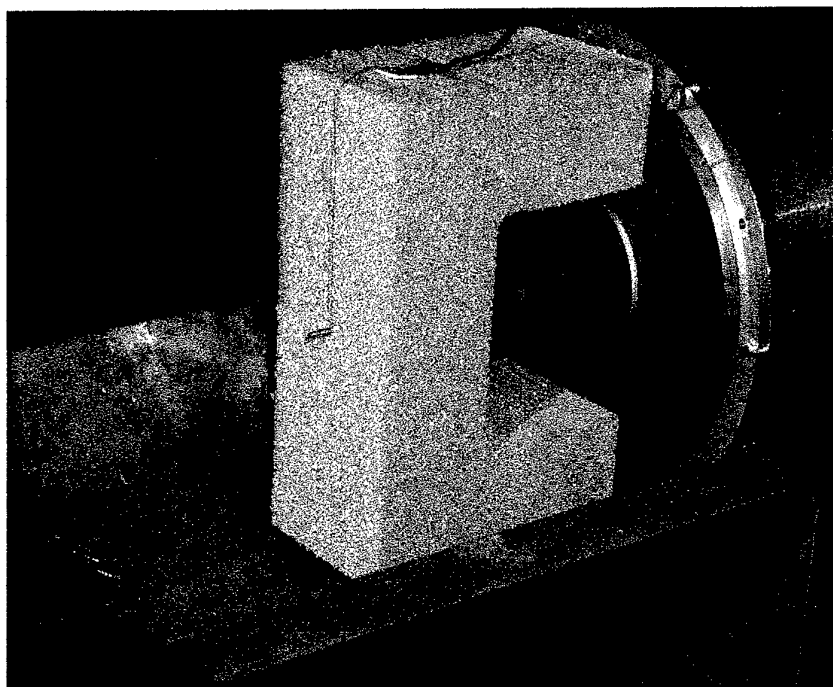
Fig. 4   Experimental set-up.

4   RESULTS

The penetration and the eroded length of the projectile versus time data are shown in Tables 3-6 and Figs. 5-12. Zero time is when the projectile hits the front cover. The penetration values listed in Tables 3-6 refer to the penetration depth in the ceramic material.

Penetration and projectile erosion velocities obtained using linear least square fits together with average projectile velocity (sum of erosion and penetration velocity) are shown in Tables 7-10. Since most of the data in Figs. 5-12 show a clear non-linear behaviour, the calculation of penetration and erosion velocity only gives the average velocities over the studied time interval. In two tests, 420 (SiC-B) and 424 (SiC-N), the impact event changed character between picture 2 and 3 (transition from interface defeat to penetration). In these two cases, only data from picture 3 and 4 are used to calculate the penetration and erosion velocities.

The evaluated penetration and projectile erosion velocities versus impact velocity are shown in Figs. 13-20. In Figs. 21-24 the sum of erosion and penetration velocity (projectile velocity) versus impact velocity is plotted. If deceleration of the projectile during penetration is negligible, the projectile velocity v should be equal to the measured impact velocity v_0.

Table 3   Penetration and projectile length data for SiC-B.

Test no.	Front cover	Impact velocity v_0 (m/s)	Time t (μs)	Penetration P (mm)	Eroded projectile length L_0-L (mm)
300	Cu	1509	11.4	0.5	13.3
			21.1	0.3	27.2
			31.9	0.2	43.3
			41.5	0.4	56.8
327	Cu	1809	10.6	1.6	10.5
			15.3	7.8	14.5
			25.8	14.0	25.6
			30.4	16.2	31.4
328	Cu	1745	10.4	1.1	10.4
			17.4	5.2	18.5
			26.9	12.2	28.0
			31.6	15.3	32.6
417	Cu	1316	11.4	0.2	7.8
			20.4	0.1	19.5
			31.7	0.1	33.8
			38.4	0.3	42.5
418	Cu	1498	11.4	0.2	9.6
			20.2	0.1	22.9
			30.6	0.2	37.8
			37.4	0.2	47.9
419	Cu	1498	11.4	0.1	10.1
			19.4	0.2	21.9
			28.4	0.2	35.4
			35.5	0.3	45.6
420	Cu	1568	10.4	0.3	7.4
			18.2	0.2	19.9
			27.4	4.2	29.9
			33.4	6.4	36.8
421	Cu	1766	9.4	0.0	7.0
			16.2	4.5	14.9
			24.4	11.1	22.6
			30.4	13.9	29.9
430	Cu	1917	9.4	0.4	8.4
			9.6	0.7	8.2
			9.8	1.1	8.8
			23.3	12.8	22.7
431	Cu	2049	8.3	0.4	7.5
			8.8	0.6	8.1
			20.4	13.0	19.8
435	Cu	1669	10.2	0.5	8.8
			11.4	0.9	10.3
			27.4	11.3	26.1
			34.4	13.9	34.8
437	Cu	1530	12.0	0.3	10.5
			20.2	0.1	23.9
			29.4	0.2	37.5
			37.4	0.1	49.4
438	Cu	2064	8.0	6.4	1.0
			9.8	9.1	2.2
			13.2	12.8	5.5
			23.4	21.9	16.8

Table 4   Penetration and projectile length data for SiC-N.

Test no.	Front cover	Impact velocity v_0 (m/s)	Time t (μs)	Penetration P (mm)	Eroded projectile length L_0-L (mm)
354	Cu	1618	10.4	0.9	11.0
			18.4	5.7	19.1
			27.6	10.3	29.2
			33.6	15.6	33.5
357	Cu	1602	11.6	0.5	12.0
			18.4	3.0	20.5
			28.6	7.9	31.6
			33.6	11.6	35.8
359	Cu	1576	11.4	0.2	10.9
			28.6	9.5	27.9
			34.8	12.3	34.8
361	Cu	1556	11.5	0.3	10.9
			19.4	5.1	18.6
			29.5	9.2	30.1
			35.6	12.9	35.8

Table 4 cont.   Penetration and projectile length data for SiC-N.

Test no.	Front cover	Impact velocity v_0 (m/s)	Time t (μs)	Penetration P (mm)	Eroded projectile length L_0-L (mm)
363	Cu	1502	11.5	0.2	10.6
			20.3	4.4	19.8
			30.4	11.2	27.9
			37.6	15.0	34.7
365	Cu	1401	12.5	0.4	11.1
			21.4	0.3	23.6
			32.6	0.3	38.7
			38.6	0.3	46.7
366	Cu	1406	12.4	0.1	9.8
			21.4	0.2	22.2
			32.5	0.1	37.3
			38.6	0.1	45.5
423	Cu	1512	11.4	0.2	9.8
			11.8	0.3	9.1
			31.4	0.2	39.3
			32.2	0.3	40.3
424	Cu	1529	11.4	0.4	9.0
			20.2	0.3	22.8
			30.4	3.4	35.0
			38.6	7.0	43.3
425	Cu	1493	11.4	0.3	9.1
			20.2	0.2	22.5
			30.4	0.2	37.4
			37.6	0.2	47.8
433	Cu	1572	19.4	4.3	18.0
			29.4	9.5	28.0
			36.5	10.7	37.9

Table 5   Penetration and projectile length data for SiC-SC-1RN.

Test no.	Front cover	Impact velocity v_0 (m/s)	Time t (μs)	Penetration P (mm)	Eroded projectile length L_0-L (mm)
356	Cu	1650	10.6	3.4	9.7
			18.4	6.8	19.5
			27.6	10.3	30.7
			33.6	14.2	36.3
358	Cu	1567	11.5	0.2	12.0
			18.4	4.7	18.2
			28.6	9.3	29.2
			34.6	12.8	35.0
360	Cu	1569	11.6	0.2	10.7
			19.3	3.1	19.8
			29.6	10.4	28.3
			35.6	14.5	33.6
364	Cu	1497	12.5	0.1	11.9
			21.4	0.3	24.8
			32.6	0.2	40.7
			38.6	0.2	49.2
368	Cu	1446	11.4	0.3	9.8
			20.4	0.4	22.7
			30.4	0.2	37.1
			37.6	0.3	46.9
369	Cu	1456	12.5	0.3	12.7
			21.4	0.1	25.6
			32.4	0.2	41.3
			38.6	0.3	49.8
426	Cu	1582	11.4	0.1	9.8
			19.2	2.9	19.3
			28.6	6.6	30.1
			35.4	12.5	34.9
427	Cu	1586	11.6	0.3	9.0
			19.2	2.5	19.2
			29.2	7.4	29.8
			36.5	9.7	38.6
428	Cu	1551	11.4	0.3	8.7
			19.2	5.7	15.8
			29.4	10.3	26.9
			36.4	12.4	35.3
436	Cu	1501	11.4	0.1	9.6
			11.6	0.1	9.9
			30.4	0.2	38.4
			11.9	0.3	10.6

Table 6 Penetration and projectile length data for SiC-HPN.

Test no.	Front cover	Impact velocity v_0 (m/s)	Time t (μs)	Penetration P (mm)	Eroded projectile length L_0-L (mm)
340	Cu	1673	10.3	0.3	11.5
			17.2	4.3	19.0
			26.8	11.3	27.8
			32.6	16.0	32.5
341	Cu	1578	11.4	0.2	10.9
			18.3	0.3	21.9
			28.8	0.2	38.4
			33.6	0.3	45.6
342	Cu	1636	10.3	0.7	9.2
			18.2	6.8	15.9
			27.6	11.7	26.8
			33.6	15.0	32.2
344	Cu	1749	10.3	1.1	9.9
			17.4	7.5	15.7
			26.6	14.8	24.7
			31.6	17.9	29.7
362	Cu	1527	11.4	0.2	10.8
			20.4	0.2	24.5
			30.4	0.1	39.8
			36.5	0.3	48.5
429	Cu	1504	20.2	0.2	23.7
			29.4	0.3	37.3
			38.1	0.4	48.7
432	Cu	1563	19.4	0.3	22.8
			20.8	0.3	24.9
			36.4	0.3	48.7
434	Cu	1613	19.4	0.1	22.9
			28.3	0.6	36.7
			35.2	0.4	47.7
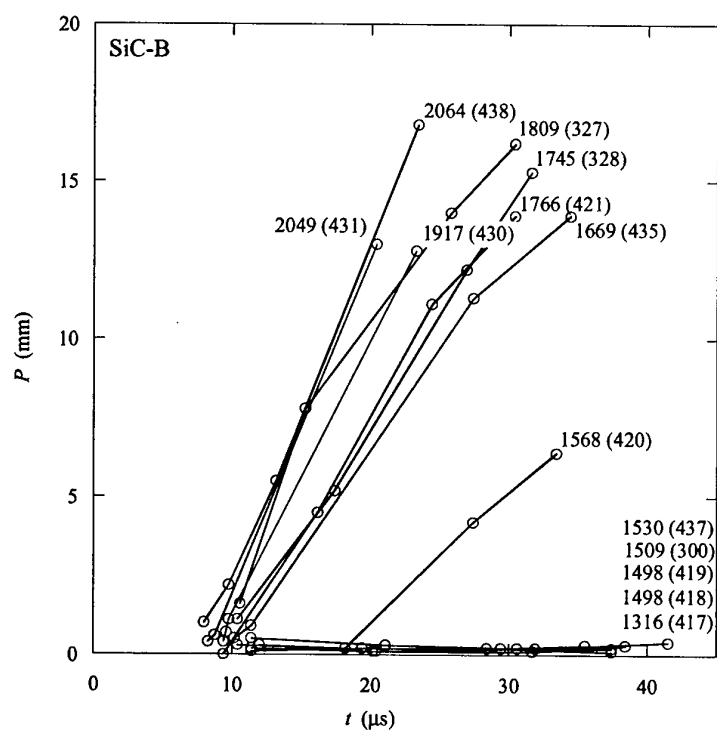
Fig. 5   Penetration P versus time t for the tests with SiC-B (indicated by impact velocity and test number).
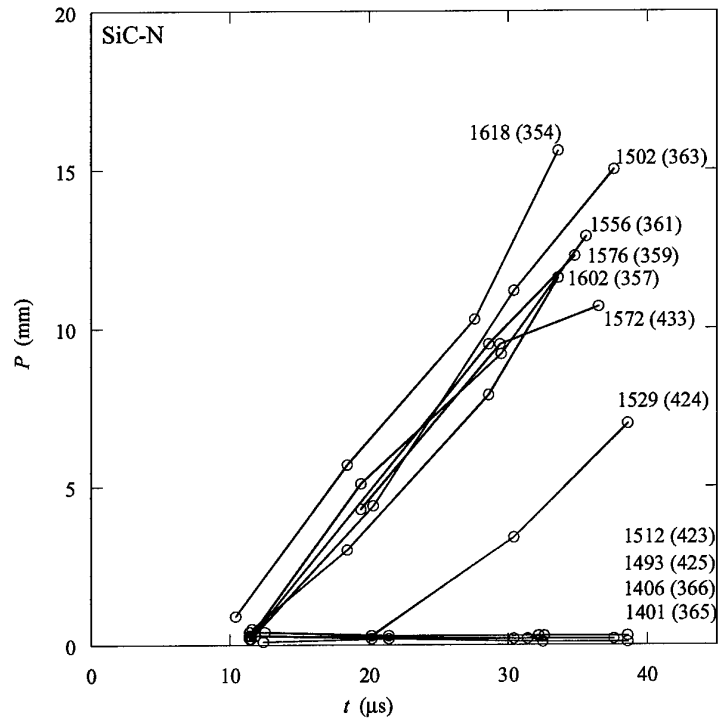
Fig. 6   Penetration P versus time t for the tests with SiC-N (indicated by impact velocity and test number).
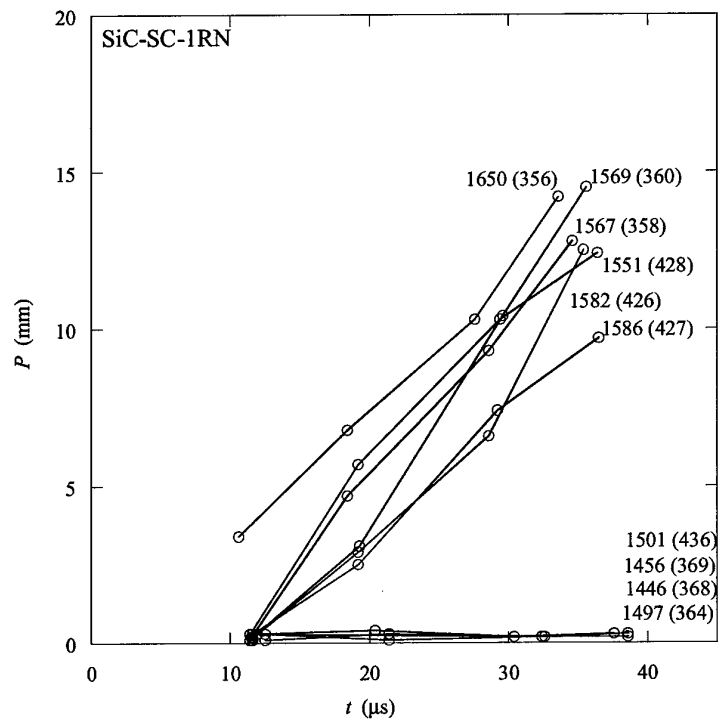
Fig. 7   Penetration P versus time t for the tests with SiC-SC-1RN (indicated by impact velocity and test number).
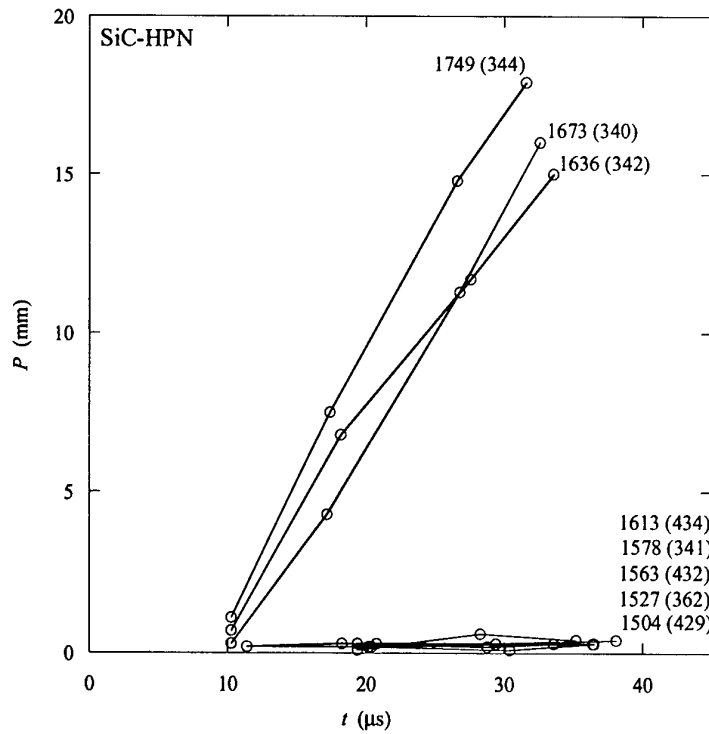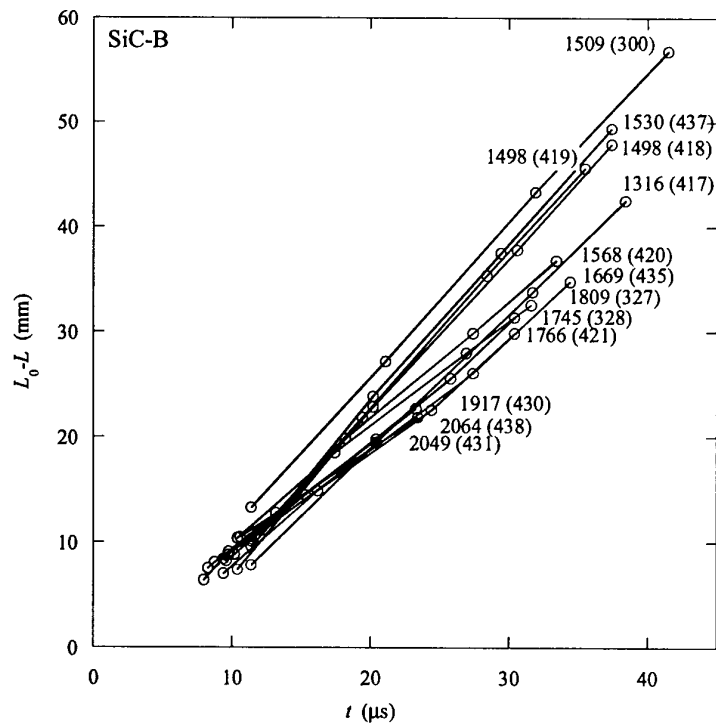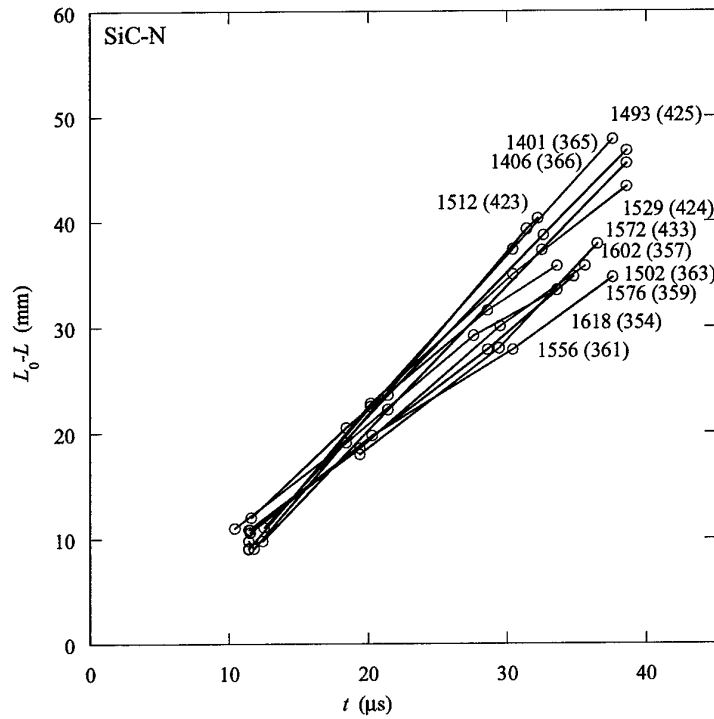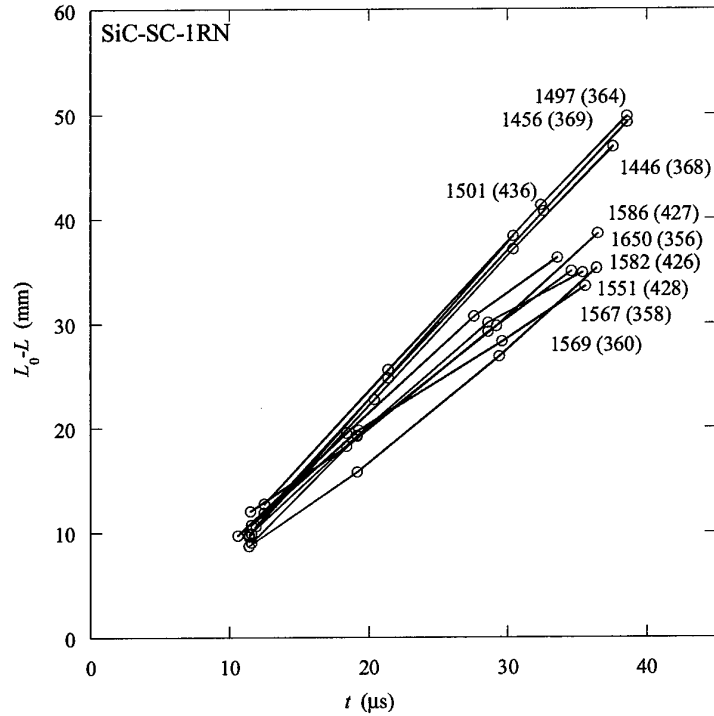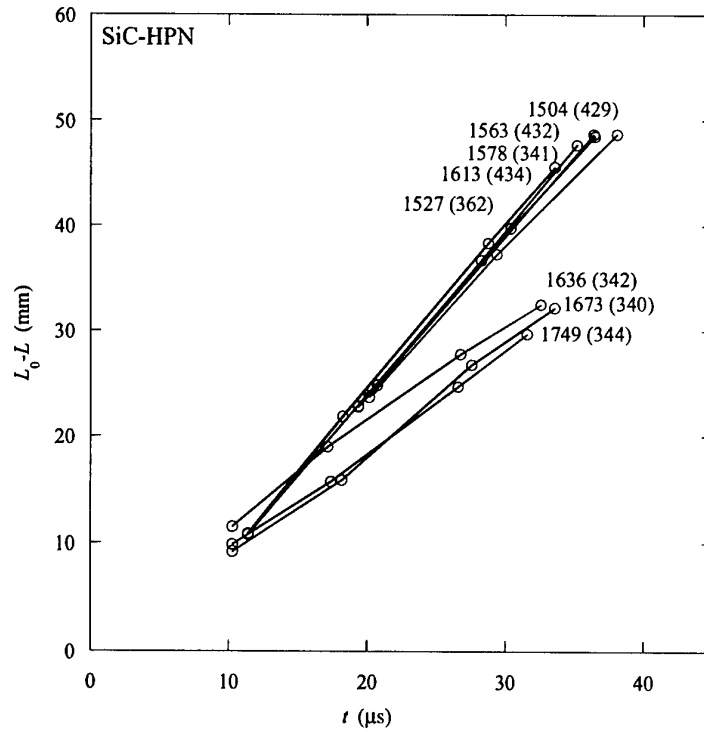
13

Fig. 8   Penetration P versus time t for the tests with SiC-HPN (indicated by impact velocity and test number).

Fig. 9   Eroded length of projectile L_0-L versus time t for the tests with SiC-B (indicated by impact velocity and test number).

Fig. 10   Eroded length of projectile L_0-L versus time t for the tests with SiC-N (indicated by impact velocity and test number).

Fig. 11   Eroded length of projectile L_0-L versus time t for the tests with SiC-SC-1RN (indicated by impact velocity and test number).

15

Fig. 12   Eroded length of projectile L_0-L versus time t for the tests with SiC-HPN (indicated by impact velocity and test number).

Table 7   Penetration and erosion velocity data for SiC-B

Test no.	Front cover	Impact velocity v_0 (m/s)	Penetration velocity, u (m/s)	Projectile erosion velocity, $\dot{L}$ (m/s)	Average projectile velocity $v = \dot{L} + u$ (m/s)
300	Cu	1509	0	1450	1450
327	Cu	1809	706	1056	1762
328	Cu	1745	680	1042	1722
417	Cu	1316	0	1282	1282
418	Cu	1498	0	1468	1468
419	Cu	1498	0	1477	1477
420	Cu	1568	367	1150	1517
421	Cu	1766	682	1070	1752
430	Cu	1917	881	1039	1920
431	Cu	2049	1054	1013	2067
435	Cu	1669	579	1052	1631
437	Cu	1530	0	1526	1526
438	Cu	2064	1046	979	2025

Table 8   Penetration and erosion velocity data for SiC-N

Test no.	Front cover	Impact velocity v_0 (m/s)	Penetration velocity, u (m/s)	Projectile erosion velocity, $\dot{L}$ (m/s)	Average projectile velocity $v = \dot{L} + u$ (m/s)
354	Cu	1618	613	990	1603
357	Cu	1602	497	1086	1583
359	Cu	1576	522	1014	1536
361	Cu	1556	506	1049	1555
363	Cu	1502	580	908	1488
365	Cu	1401	0	1362	1362
366	Cu	1406	0	1363	1363
423	Cu	1512	0	1502	1502
424	Cu	1529	439	1012	1451
425	Cu	1493	0	1476	1476
433	Cu	1572	384	1000	1384

Table 9   Penetration and erosion velocity data for SiC-SC-1RN

Test no.	Front cover	Impact velocity v_0 (m/s)	Penetration velocity, u (m/s)	Projectile erosion velocity, $\dot{L}$ (m/s)	Average projectile velocity $v = \dot{L} + u$ (m/s)
356	Cu	1650	455	1168	1623
358	Cu	1567	530	1009	1539
360	Cu	1569	611	937	1548
364	Cu	1497	0	1428	1428
368	Cu	1446	0	1420	1420
369	Cu	1456	0	1423	1423
426	Cu	1582	498	1062	1560
427	Cu	1586	393	1171	1564
428	Cu	1551	481	1066	1547
436	Cu	1501	0	1512	1512

Table 10 Penetration and erosion velocity data for SiC-HPN

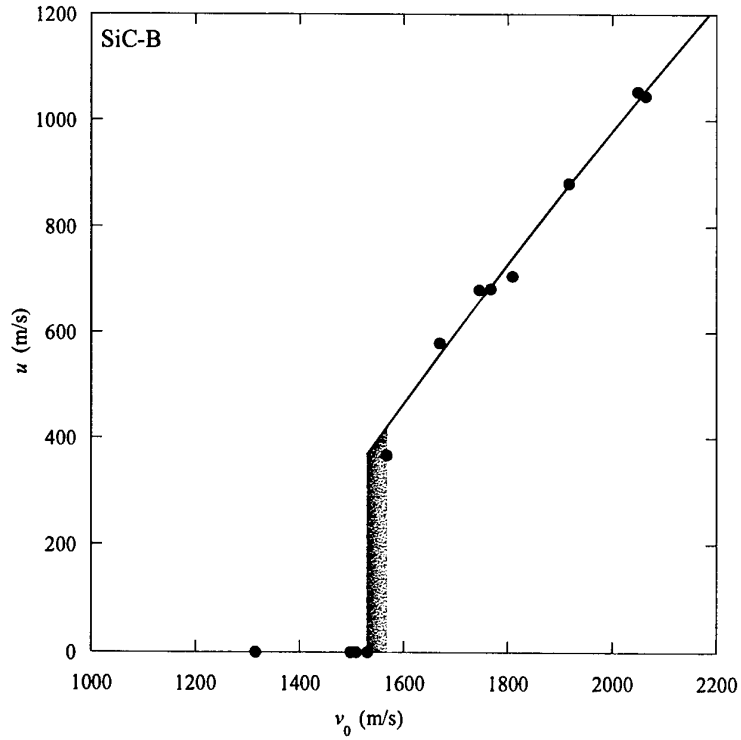| Test no.	Front cover	Impact velocity v_0 (m/s)	Penetration velocity, u (m/s)	Projectile erosion velocity, $\dot{L}$ (m/s)	Average projectile velocity $v = \dot{L} + u$ (m/s)
340	Cu	1673	708	939	1647
341	Cu	1578	0	1566	1566
342	Cu	1636	602	1010	1612
344	Cu	1749	795	935	1730
362	Cu	1527	0	1507	1507
429	Cu	1504	0	1397	1397
432	Cu	1563	0	1524	1524
434	Cu	1613	0	1569	1569

Fig. 13 Penetration velocity u versus impact velocity v_0 for the tests with SiC-B. Shaded area indicates region within which transition occurs. The solid line is a second degree fit to the penetration data.
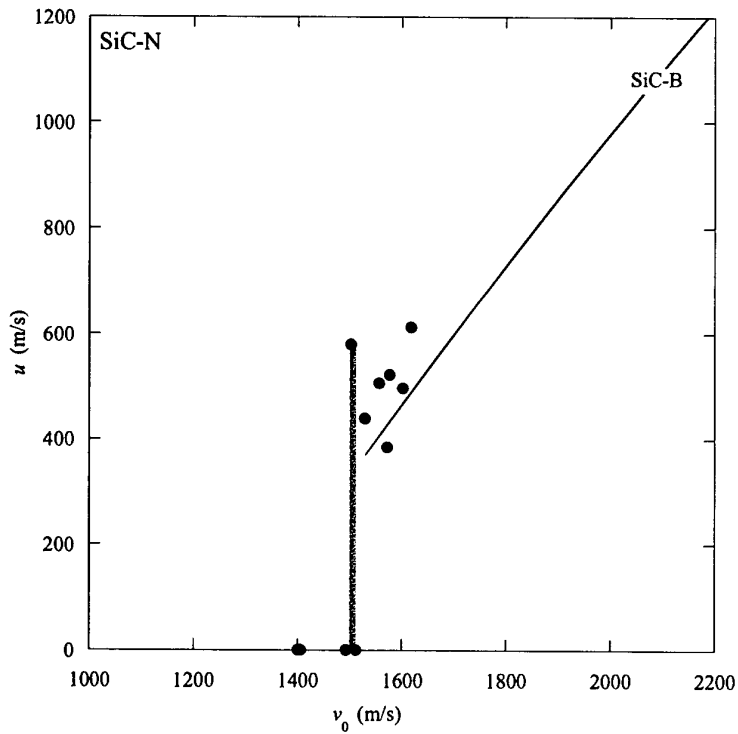

Fig. 14 Penetration velocity u versus impact velocity v_0 for the tests with SiC-N. Shaded area indicates region within which transition occurs. The solid line corresponds to the SiC-B data fit in Fig. 13.
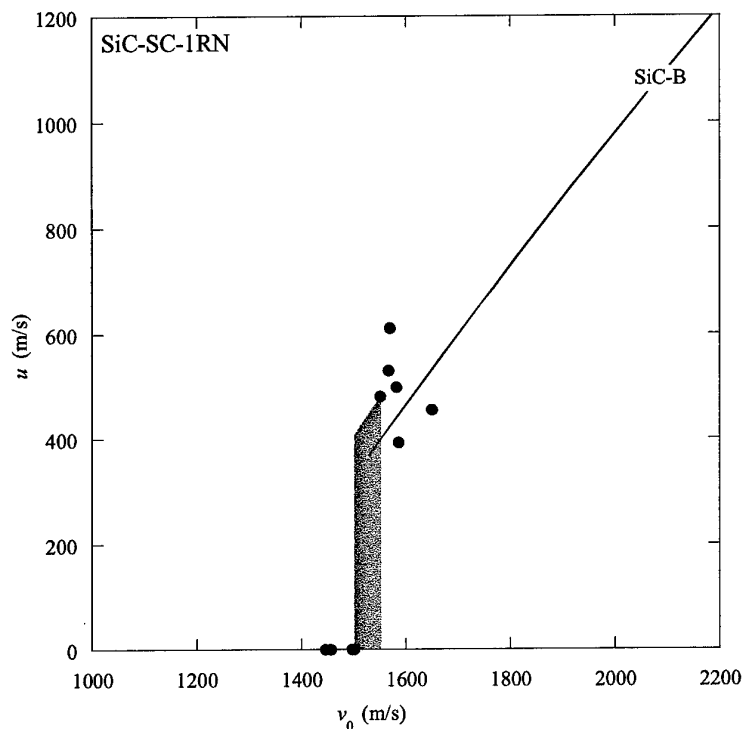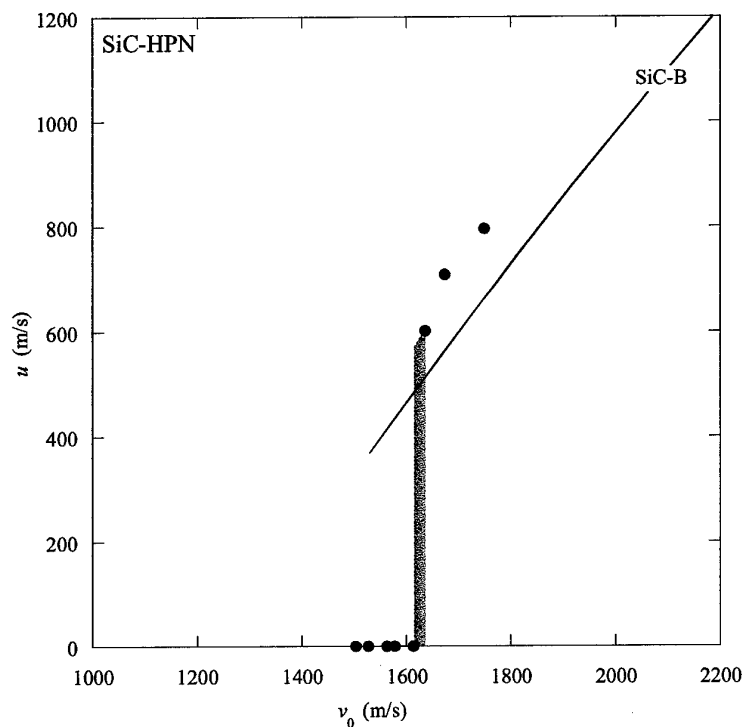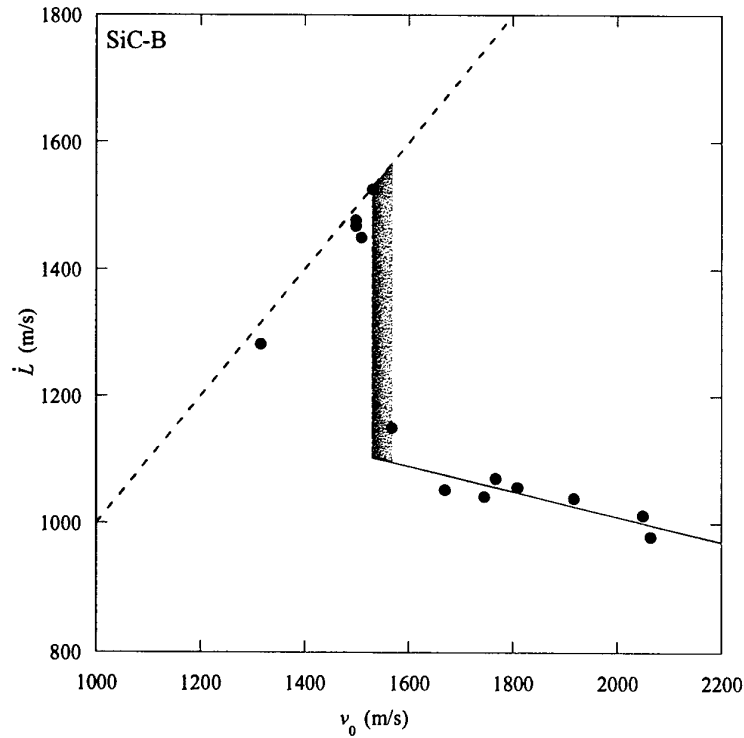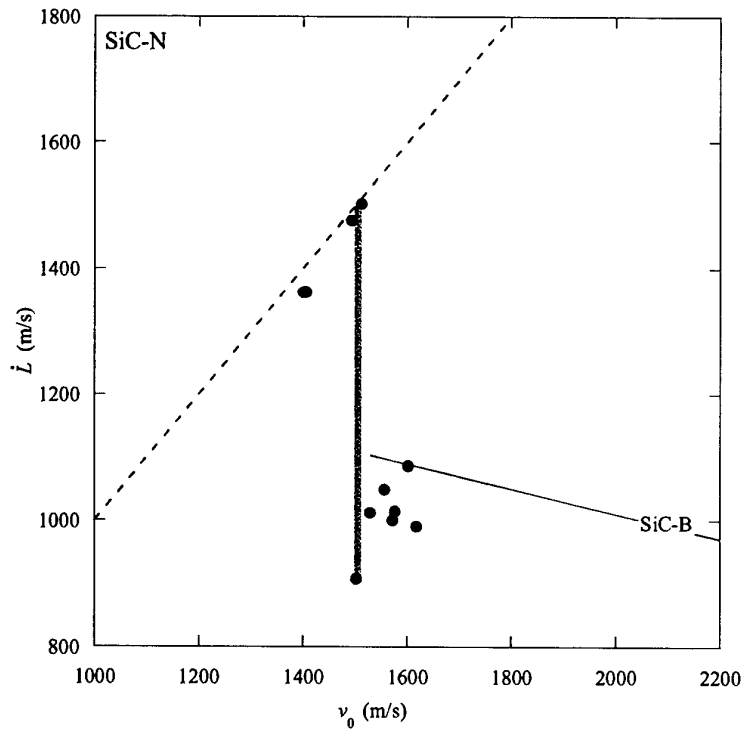
Fig. 15   Penetration velocity u versus impact velocity v_0 for the tests with SiC-SC-1RN. Shaded area indicates region within which transition occurs. The solid line corresponds to the SiC-B data fit in Fig. 13.

Fig. 16   Penetration velocity u versus impact velocity v_0 for the tests with SiC-HPN. Shaded area indicates region within which transition occurs. The solid line corresponds to the SiC-B data fit in Fig. 13.
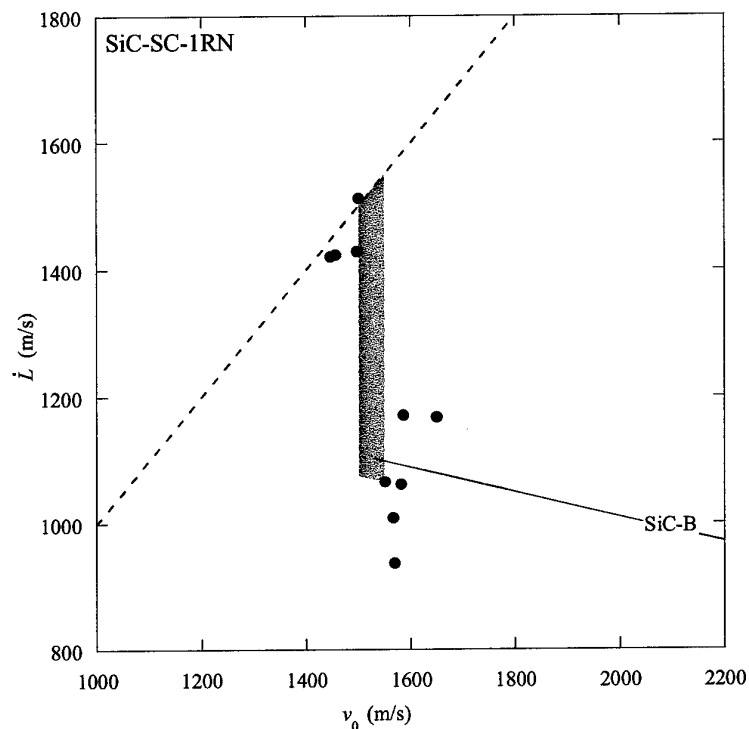
Fig. 17   Projectile erosion velocity $\dot{L}$ versus impact velocity v_0 for the tests with SiC-B. Shaded area indicates region within which transition occurs. The solid line is a second degree fit to the erosion data above the transition velocity. Dashed line represents $\dot{L} = v_0$.

Fig. 18   Projectile erosion velocity $\dot{L}$ versus impact velocity v_0 for the tests with SiC-N. Shaded area indicates region within which transition occurs. The solid line corresponds to the SiC-B data fit in Fig. 17. Dashed line represents $\dot{L} = v_0$.
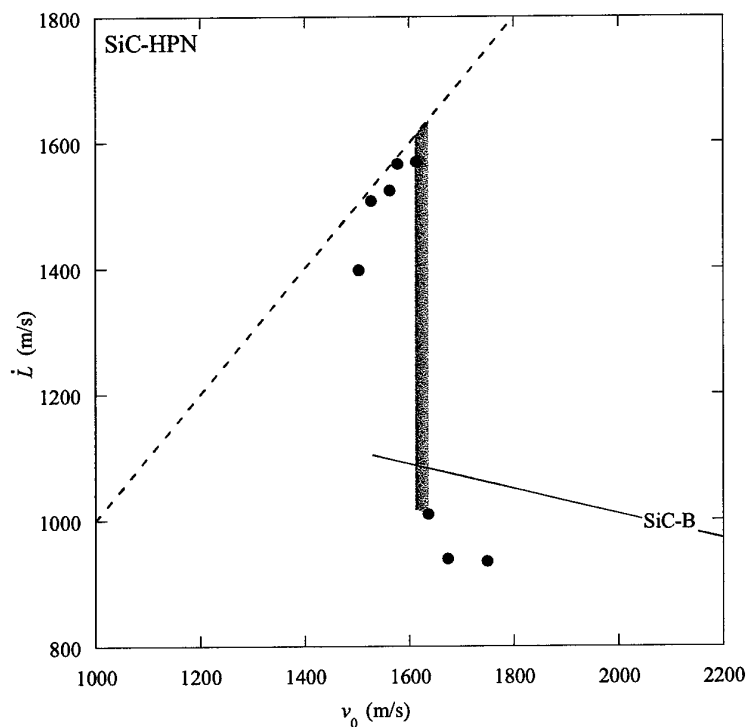
20

Fig. 19 Projectile erosion velocity $\dot{L}$ versus impact velocity v_0 for the tests with SiC-SC-1RN. Shaded area indicates region within which transition occurs. The solid line corresponds to the SiC-B data fit in Fig. 17. Dashed line represents $\dot{L} = v_0$.

Fig. 20 Projectile erosion velocity $\dot{L}$ versus impact velocity v_0 for the tests with SiC-HPN. Shaded area indicates region within which transition occurs. The solid line corresponds to the SiC-B data fit in Fig. 17. Dashed line represents $\dot{L} = v_0$.
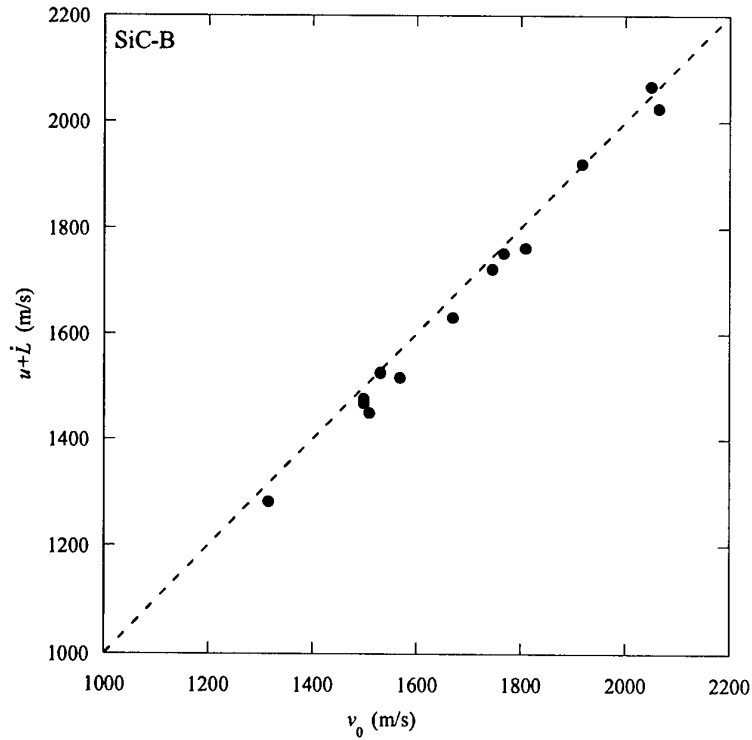
21

Fig. 21   Sum of erosion and penetration velocity (average projectile velocity) versus impact velocity for the tests with SiC-B. Dashed line represents $u + \dot{L} = v_0$.
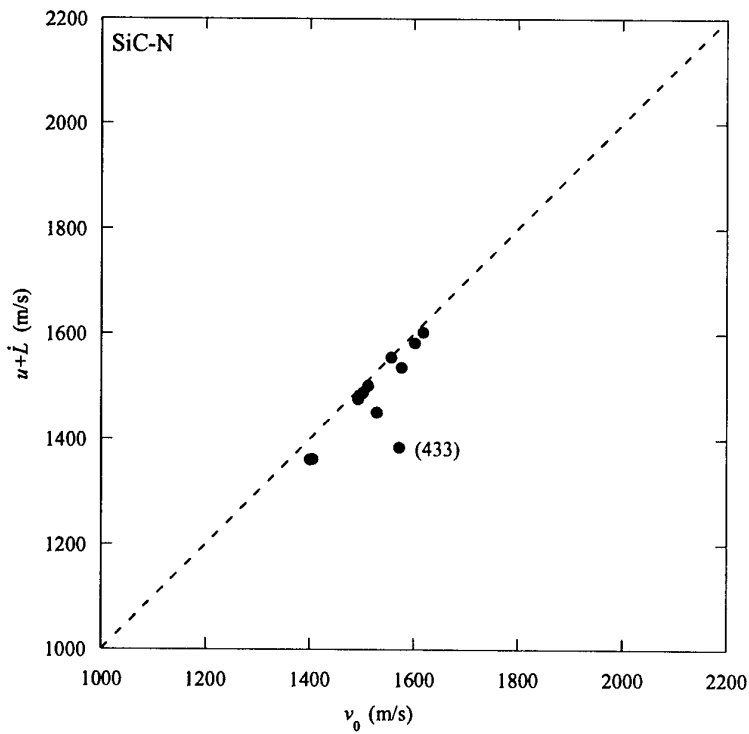

Fig. 22   Sum of erosion and penetration velocity (average projectile velocity) versus impact velocity for the tests with SiC-N. Dashed line represents $u + \dot{L} = v_0$.
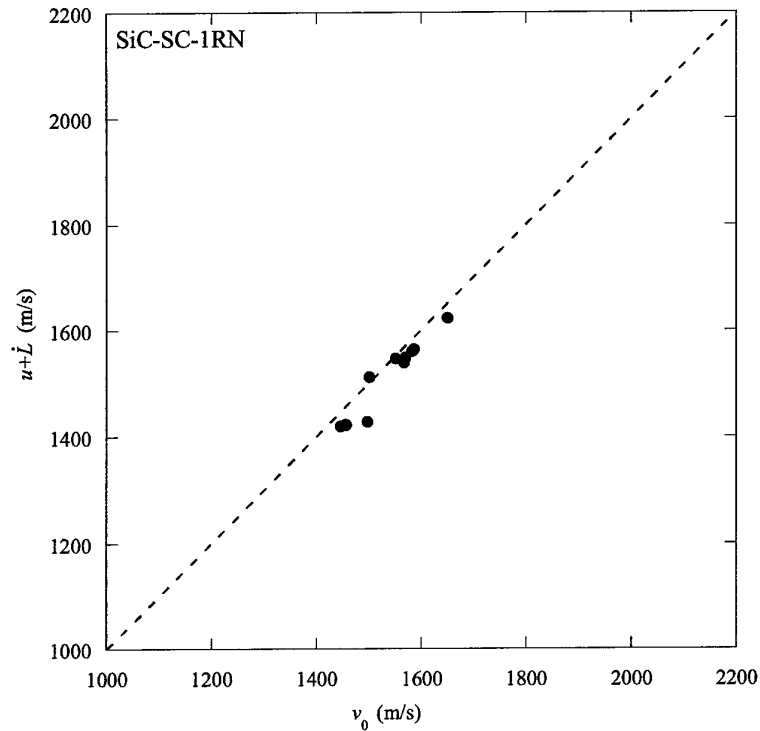
Fig. 23 Sum of erosion and penetration velocity (average projectile velocity) versus impact velocity for the tests with SiC-SC-1RN. Dashed line represents $u + \dot{L} = v_0$.
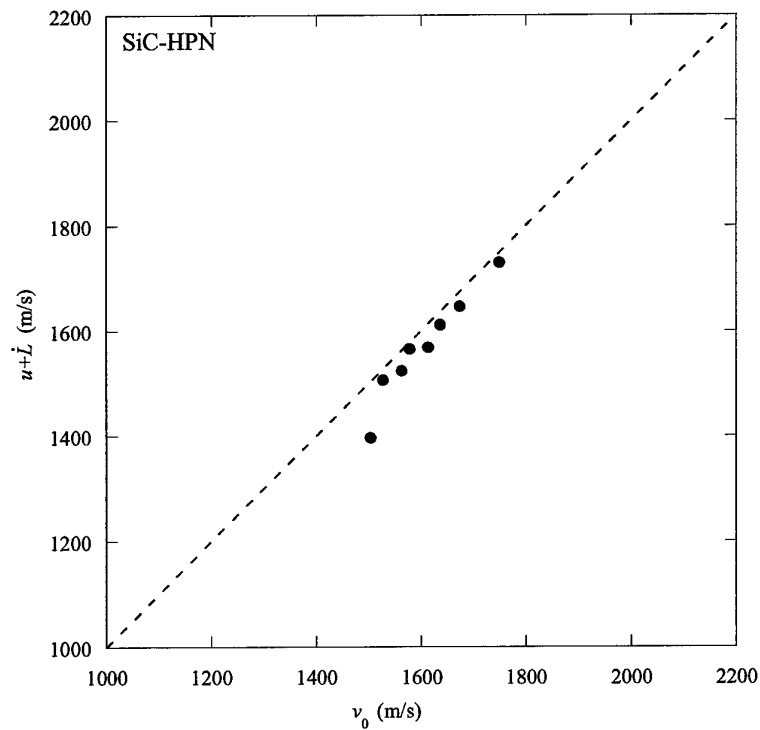

Fig. 24 Sum of erosion and penetration velocity (average projectile velocity) versus impact velocity for the tests with SiC-HPN. Dashed line represents the $u + \dot{L} = v_0$.

5 DISCUSSION

All silicon carbide materials show a distinct transition from interface defeat to penetration in this type of target configuration. The interface defeat behaviour seems to be stable, only 2 of 19 experiments which initially show interface defeat changes to penetration at a later time.

The transition velocity for each material has been determined to within 50 m/s or better. SiC-B, SiC-N and SiC-SC-1RN all show a similar transition velocity just above 1500 m/s. The highest transition velocity is for SiC-HPN, above 1600 m/s. The determined transition velocity intervals are shown in Table 11 (left and right velocities in the intervals correspond to the highest velocity without penetration and the lowest velocity with penetration, respectively).

Table 11   Transition velocity intervals

Ceramic (name)	Transition velocity intervals
SiC-B	1530-1568 ±5 m/s
SiC-N	1511-1505 ±5 m/s
SiC-SC-1RN	1501-1551 ±5 m/s
SiC-HPN	1613-1636 ±5 m/s

The penetration behaviour above the transition velocity is complicated. In several experiments, penetration seems to start normally but be interrupted after a short time. At this point the projectile material probably starts to flow radially outwards, infiltrating the conical fracture system which is formed as a result of the loading conditions. Figure 25 shows this assumed behaviour in test 433 (SiC-N). In this case it is difficult to define the actual penetration depths and projectile lengths.
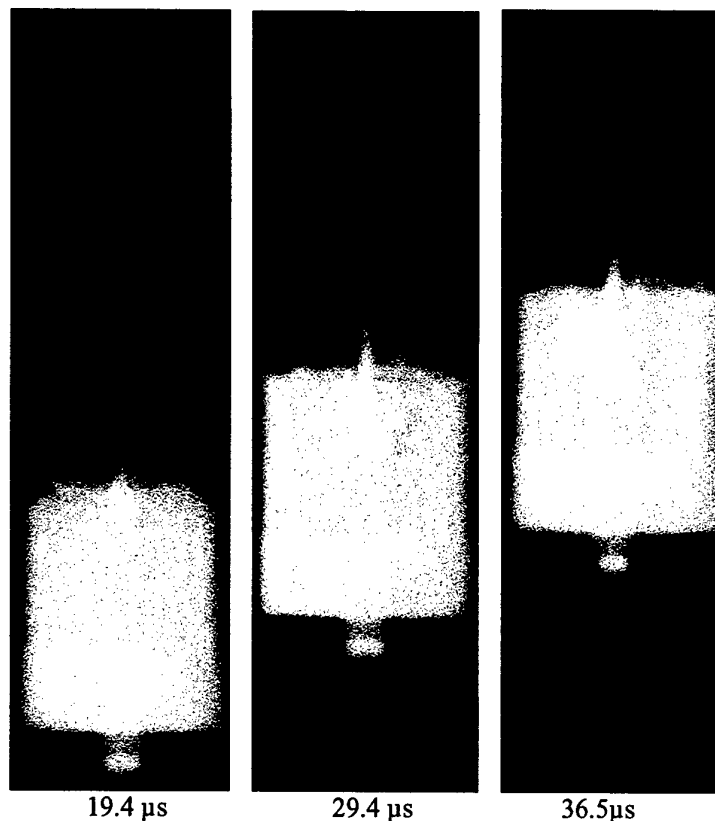

19.4 µs   29.4 µs   36.5µs

Fig. 25   Test 433 (SiC-N). The impact velocity is 1572 m/s.

This behaviour is probably the main source to the rather large scatter in the penetration- and erosion velocities for SiC-N and SiC-SC-1RN, see Figs. 14, 15 and 18, 19. Figures 13-16 show that SiC-B has the largest penetration resistance of the four materials.

6 SUGGESTIONS FOR ADDITIONAL WORK

Since the target configurations and impact conditions are the same in all tests, the only difference being the ceramic material itself, the significantly higher transition velocity for SiC-HPN compared to the other materials must be a result of different mechanical properties. It is desirable to try to find this critical mechanical property and link it to the transition velocity. These mechanical properties could possibly be found by e.g., instrumented indentation. This technique could also verify if the assumed interchange has actually taken place.

An important question in understanding the phenomenon of transition from interface defeat to penetration is the influence of the confining pressure. In the tests performed under this contract the initial confining pressure was of the order of 175 MPa. The influence of higher confining pressures on the transition velocity should be studied using the same test technique but different target design. Confining pressures on the order of 1.5 GPa should be possible to obtain and investigated using the FOI test technique. This type of work would be useful both for the interpretation of these experiments and also for evaluation of material models like the Jonnson-Holmquist JH1.

7 REFERENCES

[1] Hauver GE, Netherwood PH, Benck RF, Kecskes LJ. Ballistic performance of ceramic targets. Army Symposium on Solid Mechanics, USA, 1993

[2] Lundberg P, Holmberg L, Janzon B. An experimental study of long rod penetration into boron carbide at ordnance and hyper velocities. Proceedings of the 17th International Symposium on Ballistics, South Africa, Vol. 3, 1998. p. 251-58.

[3] Lundberg P, Renström R, Lundberg B. Impact of metallic projectiles on ceramic targets: transition between interface defeat and penetration. Int J Impact Engng 2000;24:259-275.

[4] P. Skoglund, Constitutive modelling of a tungsten heavy metal alloy. 7[Th] International conference on mechanical and physical behaviour of materials under dynamic loading. Porto, sept. 2003.

INTENTIONALLY LEFT BLANK.